Nonlinear POD-Based Reduced-Order Models for Aeroelastic Compressible Flows

Antoine Placzek, Duc-Minh Tran, Roger Ohayon

NONLINEAR POD-BASED REDUCED-ORDER MODELS FOR AEROELASTIC COMPRESSIBLE FLOWS

Antoine Placzek[1,2], Duc-Minh Tran[1] and Roger Ohayon[2]

[1]Aeroelasticity and Structural Dynamics Department, ONERA
29 av. de la Division Leclerc, BP72, 92320 Châtillon, France
antoine.placzek@onera.fr, tran@onera.fr

[2]Structural Mechanics and Coupled Systems Laboratory, CNAM
2 rue Conté, 75003 Paris, France
roger.ohayon@cnam.fr

Keywords. POD, reduced-order model, nonlinear system, Galerkin projection, Navier-Stokes equation, aeroelasticity.

Abstract. In this paper, reduced-order models (ROMs) based on the Proper Orthogonal Decomposition (POD) are developed in view of decreasing the computational cost of simulations involving fluid-structure interactions. For that purpose, a truncated POD basis is used to build two types of ROMs from the Galerkin projection of the continuous nonlinear Navier-Stokes equations. First, simulations with a classical POD-Galerkin ROM are performed to reproduce the unsteady vortex shedding process in the wake of a fixed airfoil with a large angle of attack. Then, the ROM formulation is extended to take into account the rigid body motion of the airfoil. To improve the stability, a POD-based Galerkin-free ROM is developed. The aeroelastic response of an airfoil oscillating around an equilibrium position is then reproduced at very low computational cost.

1 INTRODUCTION

Computation of complex fluid flows is nowadays a reachable task, even when transonic turbulent flows are involved in aeroelastic processes. However, the simulations are often very time consuming and only few runs can be performed although the response to different parameters is generally needed. Since the usual numerical models for the flow involve too many degrees of freedom, the solution is to replace them by *reduced-order models* (ROMs). These models mimic the behavior of the original, complex model but with significantly less degrees of freedom. For that pupose, the equations governing the system are generally projected on a suitably chosen basis which can be obtained for example from a set of solutions of the complex system. The form of the ROM is thus the same as the one of the original model and the physical properties are likely to be preserved.

In fluid dynamics, several techniques of reduced-order modeling have emerged [1, 2] and the Proper Orthogonal Decomposition (POD) has proved to be very powerful to reduce the size of nonlinear fluid dynamical systems. We therefore focus in the following on the POD method which has been widely used for incompressible flows [3–5] even if the resulting ROMs have sometimes to be carefully stabilized [6, 7]. Much less studies have been carried out for nonlinear compressible flows [2, 8, 9] because of the complexity of the equations and this is why some authors have focused on the linearized compressible equations [1, 10, 11].

In this paper, a *POD-Galerkin* ROM is firstly developed to reproduce a nonlinear compressible flow field characterized by the vortex shedding in the wake of a fixed airfoil. This

model is close to the one used in [8] but different stabilization techniques are involved here. A second POD-Galerkin ROM is then developed to take into account the rigid body motion of the airfoil but the stabilization turn out to be a difficult task. A new type of ROM called *POD-based Galerkin-free* ROM is therefore developed. Unlike the POD-Galerkin method, the coefficients of the ROM are not computed from the Galerkin projection of the continuous equation on the POD modes, but a least-squares problem is resolved to determine the best coefficients which fit the generic equation of the ROM. In this way, the long term behavior of the dynamical system is accurately reproduced.

2 FLUID FLOW MODEL

In this paper, the fluid is governed by the instantaneous Navier-Stokes equations for a Newtonian, viscous and compressible flow. For the construction of the ROM, the viscosity of the fluid is assumed to be constant and equal to a reference viscosity ($\mu = \mu_r$) and the effects of the turbulence are neglected. The Navier-Stokes equations are usually written in a conservative form using the density, the momentum and the total energy as variables. However this set of variables is not appropriate to build a ROM in the framework of a Galerkin projection because the system of equations is no longer polynomial. To avoid this problem, the isentropic Navier-Stokes equations have been used by Rowley et al. [9] since the system becomes quadratic. Iollo et al . [8] advocated the use of the modified primitive variable set $[\vartheta, \mathbf{u}, p]$, where $\vartheta = 1/\rho$ is the covolume, $\mathbf{u}$ is the vector of the velocity components and p is the pressure. With those variables, the system of equations becomes polynomial and can be written under the dimensionless form:

$$\begin{cases} \dfrac{\partial \vartheta}{\partial t} + \mathbf{u}.\nabla\vartheta = \vartheta \,\mathrm{div}\, \mathbf{u} \\ \dfrac{\partial \mathbf{u}}{\partial t} + \mathbf{u}.\nabla\mathbf{u} = -\vartheta\, \nabla p + \dfrac{1}{\mathrm{Re}}\, \vartheta \,\mathrm{div}\, \boldsymbol{\tau}_{\mu_r}(\mathbf{u}) \\ \dfrac{\partial p}{\partial t} + \mathbf{u}.\nabla p = -\gamma\, p \,\mathrm{div}\, \mathbf{u} + \dfrac{\gamma - 1}{\mathrm{Re}}\, \nabla\mathbf{u} : \boldsymbol{\tau}_{\mu_r}(\mathbf{u}) + \dfrac{\gamma}{\mathrm{Re}\,\mathrm{Pr}} \,\mathrm{div}\left(\dfrac{k_\theta}{c_v}\nabla(\vartheta\, p)\right) \end{cases} \tag{1}$$

In the previous expression, $\gamma = c_p/c_v$ is the heat capacity ratio, c_p and c_v are the specific heat capacities (under constant pressure and at constant volume respectively), k_θ is the thermal conductivity, and Re and Pr are respectively the dimensionless Reynolds and Prandtl numbers. The dimensionless viscous stress tensor $\boldsymbol{\tau}_{\mu_r}(\mathbf{u}) = \left(\nabla\mathbf{u} + \nabla\mathbf{u}^T\right) - 2/3\,(\mathrm{div}\,\mathbf{u})\,\mathbf{I}$ stem from the division of the viscous stress tensor $\boldsymbol{\tau}$ by the reference viscosity μ_r. For the second example treated in Section 4.2, the fluid is perfect and can be modeled with the Euler equations in which all the viscous terms multiplied by the inverse of the Reynolds number vanish.

Equations (1) are written in an Eulerian framework and are not adapted to take into account the motion a structure like an airfoil. If the previous equations are rewritten with the Arbitrary Lagrangian-Eulerian (ALE) formulation [12], the advective operator $\mathbf{u}.\nabla$ is modified by the relative velocity $\mathbf{c} = \mathbf{u} - \mathbf{s}$ where $\mathbf{s}$ is the velocity of the mesh points. The mesh velocity is determined to match the airfoil velocity on the airfoil surface and is null on the free boundaries. The mesh is thus deforming in the domain with an arbitrary velocity at each time step. Unfortunately this deformation is incompatible with the determination of POD modes since it requires the evaluation of temporal correlations in some *fixed* points in the space, which are generally chosen to be the mesh points. Problems arise with the ALE formulation since the same mesh point has no longer the same

fixed position in space at different time instants. The equations should be formulated on a fixed grid if a POD-based ROM is considered. This can be achieved if the structure is supposed to be *rigidly moving*: the equations are reformulated in the moving frame of reference and the mesh points are therefore seen as fixed points in the space.

The position of a point M of the mesh can be defined as $\mathbf{x} = \mathbf{x}_0 + \mathbf{R}\,\widetilde{\mathbf{x}}$, where $\mathbf{x}$ is the position of M in the absolute reference frame $\mathcal{R}_A$, $\mathbf{x}_0$ is the position of the origin M_0 of the moving frame $\mathcal{R}_E$ defined in the reference frame $\mathcal{R}_A$, $\widetilde{\mathbf{x}}$ is the position of the point M relative to M_0 in the moving frame $\mathcal{R}_E$ and $\mathbf{R}$ is the change-of-basis matrix between $\mathcal{R}_E$ and $\mathcal{R}_A$. The matrix is orthogonal ($\mathbf{R}^T\mathbf{R} = \mathbf{R}\,\mathbf{R}^T = \mathbf{I}$) and $\boldsymbol{\Omega}_A = \dot{\mathbf{R}}\,\mathbf{R}^T$ is an antisymmetric tensor describing the rotation. The angular velocity vector $\boldsymbol{\omega}_A$ is defined for all position vector $\mathbf{r} \in \mathbb{R}^3$ by $\boldsymbol{\Omega}_A\,\mathbf{r} = \boldsymbol{\omega}_A \wedge \mathbf{r}$. The velocity $\mathbf{s}$ of the mesh point M is defined by the time derivative of the position vector $\mathbf{x}$:

$$\mathbf{s}(M) = \dot{\mathbf{x}} = \underbrace{\dot{\mathbf{x}}_0 + \dot{\mathbf{R}}\,\widetilde{\mathbf{x}}}_{\mathbf{s}_e} + \underbrace{\mathbf{R}\,\dot{\widetilde{\mathbf{x}}}}_{\mathbf{s}_d} \tag{2}$$

The mesh velocity can thus be divided into two parts: the first one $\mathbf{s}_e$ is the velocity of the rigid body motion composed of the translation velocity $\mathbf{s}_0 = \dot{\mathbf{x}}_0$ and of the rotational velocity $\dot{\mathbf{R}}\,\widetilde{\mathbf{x}}$ and the second one $\mathbf{s}_d$ is the velocity associated to the deformation of the mesh. Since the airfoil is assumed to be rigidly moving, the relative position $\widetilde{\mathbf{x}}$ is time-independent and the deformation velocity $\mathbf{s}_d$ vanishes. The relative position vector can be written $\widetilde{\mathbf{x}} = \mathbf{R}^T(\mathbf{x} - \mathbf{x}_0)$ according to the definition of the absolute position vector. Introducing this relation in Eq. (2) and using the relation $\boldsymbol{\Omega}_A = \dot{\mathbf{R}}\,\mathbf{R}^T$, the mesh velocity becomes:

$$\mathbf{s}(M) = \mathbf{s}_0 + \boldsymbol{\omega}_A \wedge (\mathbf{x} - \mathbf{x}_0) \tag{3}$$

The previous relation defines the mesh velocity in the absolute frame of reference $\mathcal{R}_A$, using the coordinates of M and M_0 in the same frame. This expression could be introduced in Eq. (1) to obtain the equation governing the fluid in an absolute frame of reference where a structure is rigidly moving. However the spatial differential operators are still defined on a moving grid since the absolute position vector of the mesh points $\mathbf{x}$ changes with time. It is thus necessary to formulate the equations in the moving frame $\mathcal{R}_E$. The scalar quantities (like ϑ and p) are invariant to the reference change, unlike the vector and matrix quantities (like the velocity vector $\mathbf{u}$ and the viscous stress tensor $\boldsymbol{\tau}_{\mu_r}$). A vector $\boldsymbol{r} \in \mathbb{R}^3$ will be denoted $\mathbf{r}_A$ when its components are evaluated in the basis associated to $\mathcal{R}_A$, and $\mathbf{r}_E$ for $\mathcal{R}_E$; similarly a matrix $\boldsymbol{M} \in \mathbb{R}^3 \times \mathbb{R}^3$ is defined either in $\mathcal{R}_A$ with $\mathbf{M}_A$ or in $\mathcal{R}_E$ with $\mathbf{M}_E$. The relations between the components are obtained by means of the change-of-basis matrix $\mathbf{R}$ and additional relations are then obtained for the spatial differential operators:

$$\begin{array}{lll} \mathbf{r}_A = \mathbf{R}\,\mathbf{r}_E & \mathbf{M}_A = \mathbf{R}\,\mathbf{M}_E\,\mathbf{R}^T & \mathrm{div}_A\,\mathbf{r}_A = \mathrm{div}_E\,\mathbf{r}_E \\ \mathbf{r}_E = \mathbf{R}^T\,\mathbf{r}_A & \mathbf{M}_E = \mathbf{R}^T\,\mathbf{M}_A\,\mathbf{R} & \nabla_A\,p = \mathbf{R}\,\nabla_E\,p \end{array} \tag{4}$$

With the preceding relations, the scalar equations (for the covolume ϑ and the pressure p) can be rewritten for the absolute velocity $\mathbf{u}_E$ in the moving frame. The expression of the momentum equation in the moving frame has to be projected in $\mathcal{R}_E$ by multiplying by $\mathbf{R}^T$ since it is a vectorial equation. Besides, the time derivative of the velocity vector is given by the following formula:

$$\frac{\partial \mathbf{u}_A}{\partial t} = \frac{\delta \mathbf{u}_A}{\delta t} + \boldsymbol{\omega}_A \wedge \mathbf{u}_A \qquad \text{with} \qquad \frac{\delta \bullet}{\delta t} = \mathbf{R}\,\frac{\partial}{\partial t}\big(\mathbf{R}^T\,\bullet\big) \tag{5}$$

where $\delta/\delta t$ is the time derivative in the moving frame. The projection of the time derivative on $\mathbf{R}^T$ leads to:

$$\mathbf{R}^T \frac{\partial \mathbf{u}_A}{\partial t} = \frac{\partial \mathbf{u}_E}{\partial t} + \boldsymbol{\omega}_E \wedge \mathbf{u}_E \tag{6}$$

where a new angular velocity vector $\boldsymbol{\omega}_E$ is defined such that for all $\mathbf{r} \in \mathbb{R}^3$, $\boldsymbol{\Omega}_E \, \mathbf{r} = \boldsymbol{\omega}_E \wedge \mathbf{r}$ and $\boldsymbol{\Omega}_E = \mathbf{R}^T \boldsymbol{\Omega}_A \mathbf{R} = \mathbf{R}^T \dot{\mathbf{R}}$. Finally the expression of the Navier-Stokes equations in the moving frame reads:

$$\left\{ \begin{array}{lcl} \dfrac{\partial \vartheta}{\partial t} + (\mathbf{u}_E - \mathbf{s}_{e,E}).\nabla_E \vartheta & = & \vartheta \, \mathrm{div}_E \, \mathbf{u}_E \\ \dfrac{\partial \mathbf{u}_E}{\partial t} + (\mathbf{u}_E - \mathbf{s}_{e,E}).\nabla_E \mathbf{u}_E & = & -\vartheta \, \nabla_E \, p + \dfrac{1}{\mathrm{Re}} \, \vartheta \, \mathrm{div}_E \, \boldsymbol{\tau}_{\mu_r,E}(\mathbf{u}_E) - \boldsymbol{\omega}_E \wedge \mathbf{u}_E \\ \dfrac{\partial p}{\partial t} + (\mathbf{u}_E - \mathbf{s}_{e,E}).\nabla_E \, p & = & -\gamma \, p \, \mathrm{div}_E \, \mathbf{u}_E + \dfrac{\gamma - 1}{\mathrm{Re}} \, \nabla_E \mathbf{u}_E : \boldsymbol{\tau}_{\mu_r,E}(\mathbf{u}_E) \\ & & + \dfrac{\gamma}{\mathrm{Re}\,\mathrm{Pr}} \, \mathrm{div}_E \left(\dfrac{k_\theta}{c_v} \nabla_E (\vartheta \, p) \right) \end{array} \right. \tag{7}$$

The equations in the moving frame are just modified by the introduction of a volumic force in the momentum equation and a new convective velocity $\mathbf{u}_E - \mathbf{s}_{e,E}$. In the following, the subscript E will be dropped to simplify the notations.

Equations (1) and (7) are not intended to be resolved on a computational mesh with traditional discretization methods but they are just considered as governing equations for the ROM since the conservative formulation is not adapted in this case. Consequently, the database necessary to build the POD basis does not come directly from the resolution of Eqs (1) or (7) but from the resolution of the classical Navier-Stokes equations written with the conservative variables. A computational code like *elsA* [13] is thus adapted to generate the database and in the context of reduced-order modeling, the Navier-Stokes equations written with conservative variables and discretized with a Finite Volume technique define the so-called *high-order model*.

Equations (1) and (7) are considered under their continuous form for the construction of the ROM. The n_v modified primitive variables $\mathbf{q} = [\vartheta, \mathbf{u}, p]^T$ involved in the Navier-Stokes equations are therefore assumed to be continuous squared integrable functions on a domain $\Omega \subset \mathbb{R}^{n_d}$ ($n_d = 1, 2, 3$). The vector $\mathbf{q}$ is thus contained in the Hilbert space $H = (L^2(\Omega))^{n_v}$. In practice, the variables are only known under a discrete form by means of their degrees of freedom $\mathbf{w}$, which are an approximation of the continuous variables. Within the framework of a Finite Volume resolution of the high-order model, the degrees of freedom represent the average values of the continuous variables at the center of the N control cells of the computational mesh. Consequently the discretized variables contain $N_v = n_v N$ degrees of freedom and $\mathbf{w} \in \mathbb{R}^{N_v}$.

The Navier-Stokes equations written for a fixed domain Eq. (1) or a moving domain Eq. (7) have a polynomial form when the modified primitive variable set $\mathbf{q} = [\vartheta, \mathbf{u}, p]^T$ is adopted. The system of partial differential equations is quadratic and can be written under the generic form:

$$\dot{\mathbf{q}} = \mathbf{Q}^C(\mathbf{q}, \mathbf{q}) + \frac{1}{\mathrm{Re}} \, \mathbf{Q}^D(\mathbf{q}, \mathbf{q}) + \mathbf{T}(\mathbf{q}, \mathbf{s}_e) \tag{8}$$

where the different operators are given by:

$$\mathbf{Q}^C(\mathbf{q},\mathbf{q}) = \begin{bmatrix} -\mathbf{u}.\nabla\vartheta + \vartheta \,\mathrm{div}\, \mathbf{u} \\ -\mathbf{u}.\nabla\mathbf{u} - \vartheta\,\nabla p \\ -\mathbf{u}.\nabla p - \gamma\, p \,\mathrm{div}\, \mathbf{u} \end{bmatrix} \qquad \mathbf{T}(\mathbf{q},\mathbf{s}_e) = \begin{bmatrix} \mathbf{s}_e.\nabla\vartheta \\ \mathbf{s}_e.\nabla\mathbf{u} - \boldsymbol{\omega}\wedge\mathbf{u} \\ \mathbf{s}_e.\nabla p \end{bmatrix}$$
$$\mathbf{Q}^D(\mathbf{q},\mathbf{q}) = \begin{bmatrix} 0 \\ \vartheta \,\mathrm{div}\, \boldsymbol{\tau}_{\mu_r}(\mathbf{u}) \\ (\gamma-1)\nabla\mathbf{u} : \boldsymbol{\tau}_{\mu_r}(\mathbf{u}) + \dfrac{\gamma}{\mathrm{Pr}}\mathrm{div}\,[\nabla(\vartheta\, p)] \end{bmatrix} \tag{9}$$

The source term $\mathbf{T}$ vanishes in the case of a fixed domain. Otherwise it is a linear term for the aerodynamic variable $\mathbf{q}$ and the system becomes non-autonomous. In the following we describe how a *reduced-order model* can be developed on the basis of the preceding equations.

3 POD-BASED REDUCED-ORDER MODELS

The Proper Orthogonal Decomposition (POD) is a powerful method which provides the description of a high order system by means of a small number of elements, called the *POD modes* (POMs). These POMs contain the main features of the system response, such that the solution of the system can be reconstructed as a linear combination of the POMs. The starting point of the POD method is a set of *snapshots* describing the system and obtained either from numerical simulations with the high-order model or experiments. The set of snapshots is combined into a correlation tensor, whose properties ensure that real eigenvectors (the so-called POMs) exist. The basis containing the POMs is the best basis among all other basis of same dimension to approximate any element of the snapshots set. The POD is therefore a powerful technique for data analysis since an important database can be efficiently represented by only a small number of modes. The basis can also be used as a low-dimensional projection basis when the first POMs are kept. The Galerkin projection of the dynamical system leads to a reduced-order model whose size is equal to the number of POMs in the basis. A more detailed description of the method can be found in [14, 15] for example and a brief overview is given here.

3.1 Computation of the POD modes

Let $Q = \left\{\mathbf{q}^{(m)} \in H, m = 1, .., M\right\}$ be a finite set of snapshots, which are solutions of the high-order system at different instants $t_m \in [t_0; t_0 + T_s]$. The snapshots are assumed to be the continuous modified primitive variables $\mathbf{q} = [\vartheta, \mathbf{u}, p]^T$ and the Hilbert space $H = (L^2(\Omega))^{n_v}$ is therefore adapted to formulate the ROM. The inner product associated to the Hilbert space is defined for continuous functions:

$$\forall \mathbf{q}, \mathbf{r} \in (L^2(\Omega))^{n_v} \qquad \langle \mathbf{q}, \mathbf{r} \rangle = \int_\Omega \sum_{k=1}^{n_v} q_k\, r_k \, d\Omega \tag{10}$$

The inner product should ideally be defined such that the norm $\|\mathbf{q}\|^2 = \langle \mathbf{q}, \mathbf{q} \rangle$ represents some kind of energy of the system [9] (in the case of incompressible flows, the previous inner product represent twice the kinetic energy). For compressible flows, the total energy is not a quadratic form of the modified primitive variables and the inner product cannot represent this energy. The classical inner product for continuous functions Eq. (10) is

however adopted but the energy associated to the norm is purely mathematical. Note that the inner product is well-defined as long as the snapshots are dimensionless.

The POD consists then in finding a subspace $S \subset H$ of finite dimension $q \ll N$ which provides the best approximation of any member of Q. Usually the snapshots are *centered* and the problem is to find the best basis to approximate the snapshots $\widetilde{\mathbf{q}}^{(m)} = \mathbf{q}^{(m)} - \overline{\mathbf{q}}$, where $\overline{\mathbf{q}} = E(\mathbf{q}) = \sum_{m=1}^{M} \alpha_m \mathbf{q}^{(m)}$ is a discrete weighted temporal average, with $\alpha_m > 0$. The subspace is entirely characterized by the basis $\left\{\boldsymbol{\varphi}^{(j)} \in H, j = 1, .., q\right\}$ so that $S = \text{span}\left\{\boldsymbol{\varphi}^{(1)}, ..., \boldsymbol{\varphi}^{(q)}\right\}$. Each snapshot $\mathbf{q}^{(m)}$ can therefore be approximated on the subspace S by a linear combination of the POMs $\boldsymbol{\varphi}^{(j)}$:

$$\mathbf{q}^{(m)} = \overline{\mathbf{q}} + \sum_{j=1}^{q} a_j^{(m)} \boldsymbol{\varphi}^{(j)} \qquad \forall m \in [1; M] \tag{11}$$

The POD modes $\boldsymbol{\varphi}^{(j)}$ are solutions of the following maximization problem:

$$\max_{\boldsymbol{\varphi}^{(j)} \in H, \left\|\boldsymbol{\varphi}^{(j)}\right\| = 1} \quad E\left(\left\langle \mathbf{q}^{(m)}, \boldsymbol{\varphi}^{(j)} \right\rangle^2\right) \tag{12}$$

The previous problem is equivalent to the resolution of the eigenvalue problem $\mathscr{R}\,\boldsymbol{\varphi}^{(j)} = \lambda_j\,\boldsymbol{\varphi}^{(j)}$, where $\mathscr{R}$ is a spatial correlation tensor. Since the dimension of the correlation tensor is $N_v \times N_v$ when the discrete snapshots with N_v degrees of freedom are considered, the determination of the eigenvectors is generally too costly. A powerful variant called the *snapshots method* proposed in [16] reduces considerably the size of the eigenproblem. The method is based on the fact that the POMs are a linear combination of the snapshots:

$$\boldsymbol{\varphi}^{(j)} = \sum_{m=1}^{M} c_m^{(j)} \mathbf{q}^{(m)} \tag{13}$$

It can be shown [15, 16] that the eigenvalue problem can be transformed to obtain the small equivalent $M \times M$ problem involving the temporal correlation tensor $\mathscr{R}^*$:

$$\mathscr{R}^* \mathbf{d}^{(j)} = \lambda_j \mathbf{d}^{(j)} \tag{14}$$

where $\mathscr{R}^*_{ij} = \sqrt{\alpha_i \alpha_j}\left\langle \mathbf{q}^{(i)}, \mathbf{q}^{(j)} \right\rangle$. Once the eigenvectors $\mathbf{d}^{(j)}$ are computed, the POMs are obtained by Eq. (13) and the relation $\mathbf{c}^{(j)} = \widetilde{\boldsymbol{\alpha}} \mathbf{d}^{(j)}$, where $\widetilde{\boldsymbol{\alpha}} = \text{diag}(\sqrt{\alpha_1}, \ldots, \sqrt{\alpha_M})$.

3.2 POD-Galerkin reduced-order models

The construction of POD-Galerkin ROMs relies on the projection of the equations governing the system on the truncated POD basis which contains the most energetic modes, i.e. those associated to the greatest eigenvalues. The introduction of the POD decomposition Eq. (11) in Eq. (8) governing the dynamical system and the use of the multilinearity of the operators defined in Eqs (9) lead to:

$$\begin{aligned}
\sum_{j=1}^{q} \dot{a}_j \boldsymbol{\varphi}^{(j)} &= \mathbf{Q}^C(\overline{\mathbf{q}}, \overline{\mathbf{q}}) + \frac{1}{\text{Re}} \mathbf{Q}^D(\overline{\mathbf{q}}, \overline{\mathbf{q}}) + \mathbf{T}(\overline{\mathbf{q}}, \mathbf{s}_e) + \sum_{j=1}^{q} \mathbf{T}\left(\boldsymbol{\varphi}^{(j)}, \mathbf{s}_e\right) a_j \\
&+ \sum_{j=1}^{q} \left[\mathbf{Q}^C\left(\overline{\mathbf{q}}, \boldsymbol{\varphi}^{(j)}\right) + \mathbf{Q}^C\left(\boldsymbol{\varphi}^{(j)}, \overline{\mathbf{q}}\right) + \frac{1}{\text{Re}} \mathbf{Q}^D\left(\overline{\mathbf{q}}, \boldsymbol{\varphi}^{(j)}\right) + \frac{1}{\text{Re}} \mathbf{Q}^D\left(\boldsymbol{\varphi}^{(j)}, \overline{\mathbf{q}}\right) \right] a_j \\
&+ \sum_{j,k=1}^{q} \left[\mathbf{Q}^C\left(\boldsymbol{\varphi}^{(j)}, \boldsymbol{\varphi}^{(k)}\right) + \frac{1}{\text{Re}} \mathbf{Q}^D\left(\boldsymbol{\varphi}^{(j)}, \boldsymbol{\varphi}^{(k)}\right) \right] a_j a_k
\end{aligned} \tag{15}$$

Finally, the Galerkin projection on each orthonormal POD mode $\boldsymbol{\varphi}^{(i)}$ produces a set of q nonlinear quadratic ordinary differential equations defining the ROM:

$$\dot{a}_i = \mathcal{K}_i + \sum_{j=1}^{q} \mathcal{L}_{ij} a_j + \sum_{j,k=1}^{q} \mathcal{Q}_{jik} a_j a_k + \mathcal{K}_i^e(t) + \sum_{j=1}^{q} \mathcal{L}_{ij}^e(t) a_j \tag{16}$$

When the spatial domain is fixed, the terms $\mathcal{K}_i^e$ and $\mathcal{L}_{ij}^e$ vanish and the system is autonomous. Note that the ROM contains constant and linear terms although the Navier-Stokes equations only contain quadratic terms. This comes from the affine POD decomposition using centered snapshots. The constant, linear and quadratic coefficients defining the polynomial equations of the ROM for the fixed domain are detailed below:

$$\begin{aligned}
&\mathcal{K}_i = \mathcal{K}_i^C + \frac{1}{\mathrm{Re}}\,\mathcal{K}_i^D \quad \text{with} \quad \left\{ \begin{array}{l} \mathcal{K}_i^C = \left\langle \mathbf{Q}^C(\overline{\mathbf{q}},\overline{\mathbf{q}}), \boldsymbol{\varphi}^{(i)} \right\rangle \\ \mathcal{K}_i^D = \left\langle \mathbf{Q}^D(\overline{\mathbf{q}},\overline{\mathbf{q}}), \boldsymbol{\varphi}^{(i)} \right\rangle \end{array} \right. \\
&\mathcal{L}_{ij} = \mathcal{L}_{ij}^C + \frac{1}{\mathrm{Re}}\,\mathcal{L}_{ij}^D \quad \text{with} \quad \left\{ \begin{array}{l} \mathcal{L}_{ij}^C = \left\langle \mathbf{Q}^C\big(\overline{\mathbf{q}},\boldsymbol{\varphi}^{(j)}\big) + \mathbf{Q}^C\big(\boldsymbol{\varphi}^{(j)},\overline{\mathbf{q}}\big), \boldsymbol{\varphi}^{(i)} \right\rangle \\ \mathcal{L}_{ij}^D = \left\langle \mathbf{Q}^D\big(\overline{\mathbf{q}},\boldsymbol{\varphi}^{(j)}\big) + \mathbf{Q}^D\big(\boldsymbol{\varphi}^{(j)},\overline{\mathbf{q}}\big), \boldsymbol{\varphi}^{(i)} \right\rangle \end{array} \right. \\
&\mathcal{Q}_{ijk} = \mathcal{Q}_{ijk}^C + \frac{1}{\mathrm{Re}}\,\mathcal{Q}_{ijk}^D \quad \text{with} \quad \left\{ \begin{array}{l} \mathcal{Q}_{ijk}^C = \left\langle \mathbf{Q}^C\big(\boldsymbol{\varphi}^{(j)},\boldsymbol{\varphi}^{(k)}\big), \boldsymbol{\varphi}^{(i)} \right\rangle \\ \mathcal{Q}_{ijk}^D = \left\langle \mathbf{Q}^D\big(\boldsymbol{\varphi}^{(j)},\boldsymbol{\varphi}^{(k)}\big), \boldsymbol{\varphi}^{(i)} \right\rangle \end{array} \right.
\end{aligned} \tag{17}$$

According to Eq. (17), the detailed expression of the different coefficients only requires to develop $\mathcal{Q}_{ijk}^C$ and $\mathcal{Q}_{ijk}^D$. Indeed, the expressions of the linear (reps. constant) terms are inferred by substituting $\boldsymbol{\varphi}^{(k)}$ or $\boldsymbol{\varphi}^{(j)}$ by $\overline{\mathbf{q}}$ (resp. $\boldsymbol{\varphi}^{(k)}$ and $\boldsymbol{\varphi}^{(j)}$ by $\overline{\mathbf{q}}$). Furthermore, the vector of the POMs is divided into n_v parts corresponding to the aerodynamic variables $\boldsymbol{\varphi}^{(i)} = [\varphi_\vartheta^{(i)}, \boldsymbol{\varphi}_{\mathbf{u}}^{(i)}, \varphi_p^{(i)}]^T$, so that the expressions become:

$$\begin{aligned}
\mathcal{Q}_{ijk}^C \;=\; & -\int_\Omega \Big(\boldsymbol{\varphi}_{\mathbf{u}}^{(j)}.\nabla\varphi_\vartheta^{(k)} - \varphi_\vartheta^{(k)}\,\mathrm{div}\,\boldsymbol{\varphi}_{\mathbf{u}}^{(j)}\Big)\,\varphi_\vartheta^{(i)}\,d\Omega \\
& -\int_\Omega \Big(\boldsymbol{\varphi}_{\mathbf{u}}^{(j)}.\nabla\boldsymbol{\varphi}_{\mathbf{u}}^{(k)} + \varphi_\vartheta^{(j)}\,\nabla\varphi_p^{(k)}\Big).\boldsymbol{\varphi}_{\mathbf{u}}^{(i)}\,d\Omega \\
& -\int_\Omega \big(\boldsymbol{\varphi}_{\mathbf{u}}^{(j)}.\nabla\varphi_p^{(k)} + \gamma\,\varphi_p^{(j)}\,\mathrm{div}\,\boldsymbol{\varphi}_{\mathbf{u}}^{(k)}\big)\,\varphi_p^{(i)}\,d\Omega
\end{aligned} \tag{18}$$

$$\begin{aligned}
\mathcal{Q}_{ijk}^D \;=\; & \int_\Omega \varphi_\vartheta^{(j)}\,\mathrm{div}\,\boldsymbol{\tau}_{\mu_r}\big(\boldsymbol{\varphi}_{\mathbf{u}}^{(k)}\big).\boldsymbol{\varphi}_{\mathbf{u}}^{(i)}\,d\Omega \\
+ \; & \int_\Omega \Big[(\gamma-1)\,\nabla\boldsymbol{\varphi}_{\mathbf{u}}^{(j)} : \boldsymbol{\tau}_{\mu_r}\big(\boldsymbol{\varphi}_{\mathbf{u}}^{(k)}\big) + \frac{\gamma}{\mathrm{Pr}}\,\mathrm{div}\,\Big(\nabla\Big(\varphi_\vartheta^{(j)}\varphi_p^{(k)}\Big)\Big)\Big]\varphi_p^{(i)}\,d\Omega
\end{aligned} \tag{19}$$

The computation of the diffusive coefficient with the previous expression requires the evaluation of second order spatial derivative. To avoid this, the volumic integrals can be transformed by means of the Green-Ostrogradsky theorem and the diffusive term is therefore split into a volume and a surface contribution which are given by:

$$\begin{aligned}
\mathcal{Q}_{Vol}^D \;=\; & -\int_\Omega \varphi_\vartheta^{(j)}\,\nabla\boldsymbol{\varphi}_{\mathbf{u}}^{(i)} : \boldsymbol{\tau}_{\mu_r}\big(\boldsymbol{\varphi}_{\mathbf{u}}^{(k)}\big)d\Omega - \int_\Omega \Big(\boldsymbol{\varphi}_{\mathbf{u}}^{(i)} \otimes \nabla\varphi_\vartheta^{(j)}\Big) : \boldsymbol{\tau}_{\mu_r}\big(\boldsymbol{\varphi}_{\mathbf{u}}^{(k)}\big)d\Omega \\
& +(\gamma-1)\int_\Omega \nabla\boldsymbol{\varphi}_{\mathbf{u}}^{(j)} : \boldsymbol{\tau}_{\mu_r}\big(\boldsymbol{\varphi}_{\mathbf{u}}^{(k)}\big)\varphi_p^{(i)}\,d\Omega - \frac{\gamma}{\mathrm{Pr}}\int_\Omega \varphi_\vartheta^{(j)}\,\nabla\varphi_p^{(k)}.\nabla\varphi_p^{(i)}\,d\Omega \\
& -\frac{\gamma}{\mathrm{Pr}}\int_\Omega \varphi_p^{(k)}\,\nabla\varphi_\vartheta^{(j)}.\nabla\varphi_p^{(i)}\,d\Omega
\end{aligned} \tag{20}$$

$$\mathcal{Q}^D_{Surf} = \oint_{\partial\Omega} \left[\varphi^{(j)}_\vartheta \left(\boldsymbol{\varphi}^{(i)}_{\mathbf{u}}\right)^T \boldsymbol{\tau}\left(\boldsymbol{\varphi}^{(k)}_{\mathbf{u}}\right)\right].\mathbf{n}\, d\partial\Omega + \frac{\gamma}{\mathrm{Pr}} \oint_{\partial\Omega} \varphi^{(i)}_p \nabla\left(\varphi^{(j)}_\vartheta \varphi^{(k)}_p\right).\mathbf{n}\, d\partial\Omega \quad (21)$$

When the domain is rigidly moving, additional terms have to be taken into account in the ROM. The expression of the linear moving frame coefficient is given below (the expression of the constant term is obtained by replacing $\boldsymbol{\varphi}^{(j)}$ by $\overline{\mathbf{q}}$):

$$\begin{aligned}\mathcal{L}^e_{ij}(t) &= \int_\Omega \left(\mathbf{s}_{e,E}(t).\nabla\varphi^{(j)}_\vartheta\right)\varphi^{(i)}_\vartheta\, d\Omega + \int_\Omega \left(\mathbf{s}_{e,E}(t).\nabla\varphi^{(j)}_p\right)\varphi^{(i)}_p\, d\Omega \\ &+ \int_\Omega \left(\mathbf{s}_{e,E}(t).\nabla\boldsymbol{\varphi}^{(j)}_{\mathbf{u}} - \boldsymbol{\omega}_E(t)\wedge\boldsymbol{\varphi}^{(j)}_{\mathbf{u}}\right).\boldsymbol{\varphi}^{(i)}_{\mathbf{u}}\, d\Omega\end{aligned} \quad (22)$$

These terms make the system become non-autonomous because the mesh velocity $\mathbf{s}_{e,E}$, and consequently the moving frame coefficients $\mathcal{K}^e_i$ and $\mathcal{L}^e_{ij}$, are time-dependent. The expression Eq. (22) is not adapted since the translation and rotational velocities which describe the airfoil motion appear implicitly. This means that the motion applied to the airfoil could not be changed in the ROM unless the moving frame coefficients are recalculated at each time step. This would be very costly because it involves vectors of dimension N_v. The expression has thus to be modified so that the velocities of the airfoil appear explicitly in the ROM.

The prescribed motion is described by the mesh velocity $\mathbf{s}_e = \mathbf{s}_{0,E} + \boldsymbol{\omega}_E \wedge \widetilde{\mathbf{x}}$. More precisely, the rigid body motion is governed by two degrees of freedom which are the translation velocity $\mathbf{s}_{0,E}$ and the rotational velocity $\boldsymbol{\omega}_E$. These two parameters are independent of the spatial position and can therefore be extracted from the volume integrals involved in the expression Eq. (22) of the moving frame coefficients. The relative position $\widetilde{\mathbf{x}}$ is on the contrary position-dependent, but since a rigid body motion is assumed, $\widetilde{\mathbf{x}}$ is time-independent. Consequently there is a natural space-time separation and the expression of the coefficients can be transformed so that time-independent coefficients which are then multiplied by the motion parameters can be obtained. The constant and linear moving frame coefficients can be written as follows:

$$\mathcal{K}^e_i(t) = \mathbf{s}_{0,E}(t).\boldsymbol{\mathcal{K}}^{e,T}_i + \boldsymbol{\omega}_E(t).\boldsymbol{\mathcal{K}}^{e,R}_i \quad (23)$$

$$\mathcal{L}^e_{ij}(t) = \mathbf{s}_{0,E}(t).\boldsymbol{\mathcal{L}}^{e,T}_{ij} + \boldsymbol{\omega}_E(t).\boldsymbol{\mathcal{L}}^{e,R}_{ij} \quad (24)$$

The moving frame coefficients are split into two parts relative to the translational and the rotational degrees of freedom for the rigid body motion. For each mode $\boldsymbol{\varphi}^{(i)}$, a three components vector $\boldsymbol{\mathcal{K}}^{e,T}_i$ (resp. $\boldsymbol{\mathcal{K}}^{e,R}_i$) must be computed for the constant contribution. These new coefficients are time-independent and can be computed once for all before the time integration of the ROM. The same procedure is carried out for the linear moving frame coefficient. In this way, the translational and rotational velocities of the rigid body motion can be changed in the ROM ad libitum without computing again the coefficients. The detailed expression of the translational and rotational linear moving frame coefficients are given below (the expression of the constant term is obtained by replacing $\boldsymbol{\varphi}^{(j)}$ by $\overline{\mathbf{q}}$):

$$\mathcal{L}^{e,T}_{ij} = \int_\Omega \varphi^{(i)}_\vartheta \nabla\varphi^{(j)}_\vartheta\, d\Omega + \int_\Omega \varphi^{(i)}_p \nabla\varphi^{(j)}_p\, d\Omega + \int_\Omega \left[\left(\boldsymbol{\varphi}^{(i)}_{\mathbf{u}}\right)^T \nabla\boldsymbol{\varphi}^{(j)}_{\mathbf{u}}\right]^T d\Omega \quad (25)$$

$$\begin{aligned}\mathcal{L}^{e,R}_{ij} &= \int_\Omega \left(\widetilde{\mathbf{x}}\wedge\nabla\varphi^{(j)}_\vartheta\right)\varphi^{(i)}_\vartheta\, d\Omega + \int_\Omega \left(\widetilde{\mathbf{x}}\wedge\nabla\varphi^{(j)}_p\right)\varphi^{(i)}_p\, d\Omega \\ &+ \int_\Omega \widetilde{\mathbf{x}}\wedge\left[\left(\boldsymbol{\varphi}^{(i)}_{\mathbf{u}}\right)^T\nabla\boldsymbol{\varphi}^{(j)}_{\mathbf{u}}\right]^T d\Omega - \int_\Omega \boldsymbol{\varphi}^{(j)}_{\mathbf{u}}\wedge\boldsymbol{\varphi}^{(i)}_{\mathbf{u}}\, d\Omega\end{aligned} \quad (26)$$

The POD-Galerkin procedure provides a ROM which preserves the nonlinearities of the original high order model. For a fixed domain, the ROM is given by Eq. (16) without the unsteady coefficients $\mathcal{K}_i^e$ and $\mathcal{L}_{ij}^e$. The coefficients are defined by Eqs. (17) and detailed in Eqs (18), (20) and (21). When q basis vectors are used in the projection basis, the ROM requires the computation of $q + q^2 + q^3$ coefficients. For a rigidly moving frame, the formulation of the Navier-Stokes equations in the moving frame leads to the ROM Eq. (16) including all the coefficients and the moving frame coefficients are defined by Eqs (23) and (24) and detailed in Eqs (25) and (26). In this case, the ROM is defined by $6q + 6q^2$ additional coefficients.

POD-Galerkin ROMs are able to reproduce accurately the system response but they often lack stabilization [4–7]. This can be due to the truncation of the POD basis, to the non-respect of certain boundary conditions by the POMs, or to numerical errors. Many stabilization techniques have been developed to correct the damping of the system. Amongst them, those using the exact modal amplitudes $\mathbf{a}^e$ associated to the POD decomposition Eq. (11) of the snapshots over the time interval $[t_0; t_0 + T_s]$ are often able to provide a robust stabilization. The modal amplitudes also contain important information regarding the system because the POD can be regarded as a Singular Value Decomposition (SVD) of the correlation tensor: the POMs are thus the left singular vectors and the modal amplitudes are the right ones. Cazemier et al . [5] introduced a linear diagonal correction term defined in such a way that the average energy of the modal amplitudes is conserved over the time interval. To improve this correction, Couplet et al . [6] defined an optimization problem to calibrate some chosen coefficients of the ROM so that the response of the ROM match the exact modal amplitudes on the sampling time interval $[t_0; t_0 + T_s]$. In this case, constant, linear and even quadratic coefficients can be corrected. These calibration techniques improve considerably the short-term response of the system but some kind of divergence occurs sometimes in long-term simulations [7].

3.3 POD-based Galerkin-free reduced-order models

POD-Galerkin ROMs are sometimes unable to reproduce correctly the long-term behavior of the high order model. Moreover, the computation of the coefficients becomes very time-consuming when the number of degrees of freedom of the high order model and the size of the projection basis increase. To avoid these problems, POD-based Galerkin-free methods can be used [17]. The philosophy is different from the POD-Galerkin method since the coefficients are not directly computed from the inner products of the Galerkin projection, but they are found as the solution of a least-squares problem: given the generic form of the ROM and the exact modal amplitudes associated to the POMs computed, the coefficients are determined to match the exact response.

Since the form of the ROM has already been established in the previous section, the coefficients are sought in the following to fit the response produced by Eq. (16) to the exact response but another type of equations (linear, cubic polynomials,...) could be considered. The method is called *Galerkin-free* since the equation to fit can be chosen independently of the equation governing actually the system. The procedure is described here for a fixed domain for simplicity but it can be easily extended to a moving domain.

Given the exact modal amplitudes and their time derivatives, M relations can be written with Eq. (16) at each time instant t_m. The problem is then, for each POM $\boldsymbol{\varphi}^{(i)}$, to find the vector $\mathbf{X}_i$ containing the $1 + q + q^2$ coefficients corresponding to the i-th equation of the ROM such that $\boldsymbol{\mathcal{A}}_i \mathbf{X}_i = \boldsymbol{\mathcal{B}}_i$. The matrix $\boldsymbol{\mathcal{A}}_i$ contains the exact modal amplitudes

and the correlations involved in generic polynomial equations (16) which are going to be fitted and $\boldsymbol{\mathcal{B}}_i$ is the time derivative of the i-th modal amplitude at each time instant t_m:

$$\boldsymbol{\mathcal{A}}_i = \begin{bmatrix} 1 & \cdots & a_i(t_1) & \cdots & a_i(t_1)a_j(t_1) & \cdots \\ \vdots & & \vdots & & \vdots & \\ 1 & \cdots & a_i(t_M) & \cdots & a_i(t_M)a_j(t_M) & \cdots \end{bmatrix} \quad \mathbf{X}_i = \begin{bmatrix} \mathcal{K}_i \\ \mathcal{L}_{ij} \\ \mathcal{Q}_{ijk} \end{bmatrix} \quad \boldsymbol{\mathcal{B}}_i = \begin{bmatrix} \dot{a}_i(t_1) \\ \vdots \\ \dot{a}_i(t_M) \end{bmatrix} \tag{27}$$

The matrix $\boldsymbol{\mathcal{A}}_i$ is not invertible since the problem is generally over-determined ($M > 1+q+q^2$) and the problem can only be approximated. A simple least-squares minimization procedure provides the following estimation of the coefficients: $\mathbf{X}_i = \left(\boldsymbol{\mathcal{A}_i}^T \boldsymbol{\mathcal{A}_i}\right)^{-1} \boldsymbol{\mathcal{A}_i}^T \boldsymbol{\mathcal{B}_i}$. The results is generally not accurate because the matrix $\boldsymbol{\mathcal{A}}_i$ is ill-conditioned and the smallest singular values lead to spurious results. A better solution consists in computing a truncated singular value decomposition (TSVD) of $\boldsymbol{\mathcal{A}}_i$ in which the smallest singular values have been neglected. Then the approximated pseudo-inverse matrix $\boldsymbol{\mathcal{A}}_i^+$ is computed and coefficients obtained with $\mathbf{X}_i = \boldsymbol{\mathcal{A}}_i^+ \boldsymbol{\mathcal{B}}_i$ are much better.

4 NUMERICAL APPLICATIONS

Reduced-order models of the Navier-Stokes and Euler equations are constructed in order to reproduce the aerodynamic forces applied on a fixed or a rigidly moving airfoil. In the first case, the domain is fixed and the flow field over the airfoil generates a vortex street in the wake, which causes the unsteadiness of the aerodynamic forces. In the second case, the forces oscillate because of the rigid body motion applied to the airfoil.

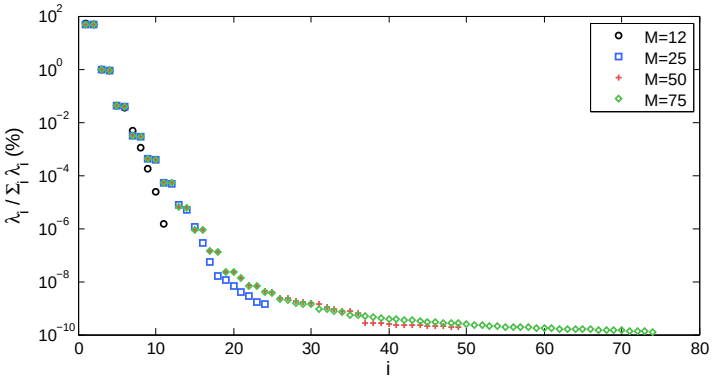

Figure 1: Percentage of energy captured by each eigenvalue λ_i associated to the POM $\boldsymbol{\varphi}^{(i)}$ computed for the NACA0012 example. Several dimensions M of the snapshots set are investigated.

4.1 Vortex shedding in the wake of a fixed NACA0012 airfoil

The first example is close to the one treated in [8], where the aerodynamic 2D flow around a NACA0012 is considered. The flow is assumed to be subsonic (Ma = 0.2) and laminar (Re = 2000) so that no turbulence closure model is necessary. The angle of attack is set to $\alpha = 20^\circ$ to observe the vortex street in the wake. Snapshots are generated over about one period of vortex shedding by means of the resolution of the Navier-Stokes equations with Onera's CFD software *elsA* [13]. The simulation with the high-order model is performed in a conservative framework but the variables extracted at each time instant t_m are the dimensionless modified primitive variables $\mathbf{q} = [\vartheta, \mathbf{u}, p]^T$.

The percentage of energy captured by each POM is represented on Figure 1 for different numbers of snapshots extracted on the same time interval $[t_0; t_0 + T_s]$ after the transient

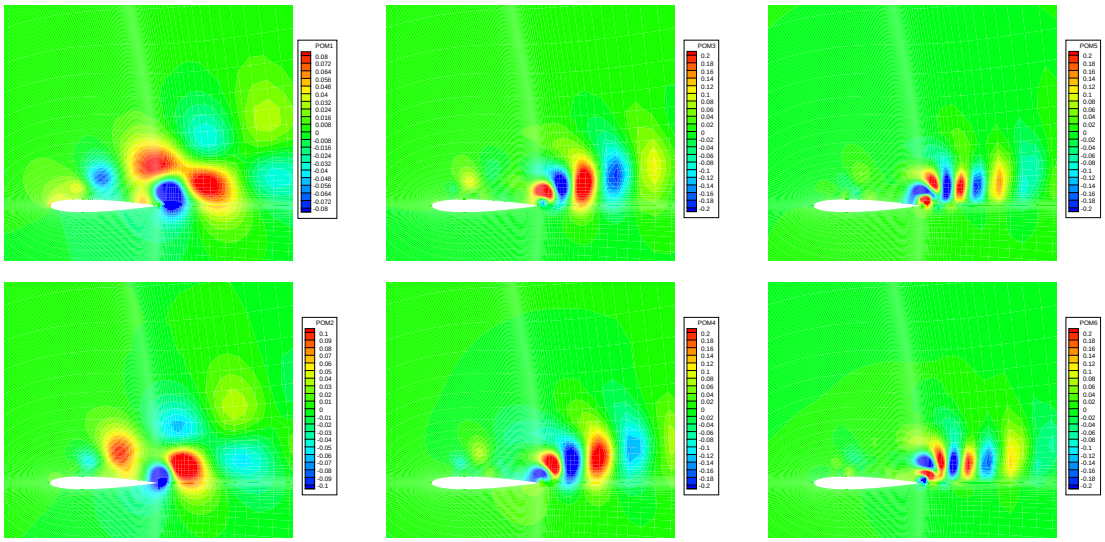

Figure 2: Shape of the first six pressure POMs $\varphi_p^{(i)}$ $(i = 1, \ldots, 6)$ of the flow field around the NACA0012 airfoil. $M = 50$ snapshots have been used.

vanishes. The first-ever POMs contain almost the totality of the energy: the cumulated percentage of energy $\eta_q = \sum_{i=1}^{q} \lambda_i / \sum_{i=1}^{M} \lambda_i$ with only $q = 6$ POMs is equal to 99.99% and is almost 100% with $q = 10$ POMs. The number of snapshots used has little influence on the spectrum and in the following, only $M = 50$ snapshots are used. The first six POMs for the pressure are represented on Figure 2. It can be seen that the POMs are grouped by pairs and that the size of the coherent structures appearing in each POM is decreasing when the number i of the POM increases.

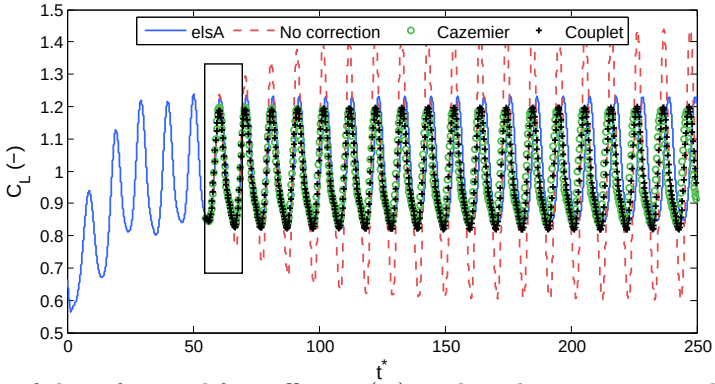

Figure 3: Comparison of the reference lift coefficient $(-)$ to the solutions computed with the ROM without correction $(--)$, with the correction of Cazemier et al. [5] $(\circ)$ and with the calibration procedure inspired by the one of Couplet et al. [6] $(+)$.

A POD-Galerkin ROM is constructed with 10 POMs so that almost all of the energy is contained in the projection basis. The short term behavior of the ROM response (i.e. the response on the sampling time interval $[t_0; t_0 + T_s]$) is quite satisfactory: the red curve of the lift coefficient on the plot Figure 3 matches the reference curve in blue which stem from the high order model simulation. However, outside the black rectangle representing the sampling time interval, the response of the ROM lacks dissipation and the lift coefficient reaches another limit cycle. This lack of damping can not reasonably be attributed to the truncation of the POD basis since the energy lost by the truncation $\varepsilon_q = 1 - \eta_q$ is less than $10^{-4}\%$ with $q = 10$. The reason is probably due to the absence of artificial dissipation in the ROM unlike the high order model. The artificial dissipation operator

has not been included in the ROM because its form is not adapted to a POD decomposition. The solution is thus to correct the ROM by means of the exact modal amplitudes: two corrections based on those proposed in [5] and [6] are used here. In the first case, only the linear diagonal terms are modified so that the energy of the modal amplitude is conserved. In the second case, the constant and linear diagonal coefficients are calibrated.

The POD-Galerkin ROM of the aerodynamic flow field constructed here is able to reproduce accurately the aerodynamic force in only several seconds. The time gain (ratio of the time integration of the high order model over the one of the reduced order model) given in the last column of Table 1 is significant. However, the construction of the ROM is costly, particularly when the correction of Couplet et al. [6] is adopted.

ROM	Construction	Time integration	Time gain
NACA0012 (correction [5])	5060	6.7	187
NACA0012 (correction [6])	8250	8.8	143
NACA0064 (POD-Galerkin `KdL`)	10598	11.8	33
NACA0064 (POD-Galerkin `K3dL`)	12326	7.3	50
NACA0064 (POD-Galerkin `KdL_E`)	18558	7.8	53
NACA0064 (Galerkin-free)	1503	4.9	80

Table 1: CPU times (in seconds) for the construction and the time integration of the different ROMs and comparison with the CPU times of the high order model.

4.2 Transonic flow around a NACA0064 oscillating airfoil

In the second example, a rigid body motion is applied to a NACA0064 airfoil. The flow is assumed to be perfect (no viscous term) and compressible (Ma = 0.796). The airfoil is subjected to a translational motion at a constant horizontal velocity V_∞ and a rotational motion such that the pitch angle α oscillates at the reduced frequency $k_{\text{red}} = \omega_\alpha / V_\infty$. The rotational motion is described by the pitch angle $\alpha(t) = \alpha_0 + \alpha_m \sin(\omega_\alpha t)$, where $\alpha_0 = 0$ and $\alpha_m = -1.0$. The translational velocity $\mathbf{s}_{e,E}$ and the angular velocity $\boldsymbol{\omega}_E$ are given by:

$$\mathbf{s}_{e,E} = V_\infty \begin{bmatrix} \cos\alpha(t) \\ 0 \\ \sin\alpha(t) \end{bmatrix} \qquad \boldsymbol{\omega}_E = \begin{bmatrix} 0 \\ \dot{\alpha}(t) \\ 0 \end{bmatrix} \tag{28}$$

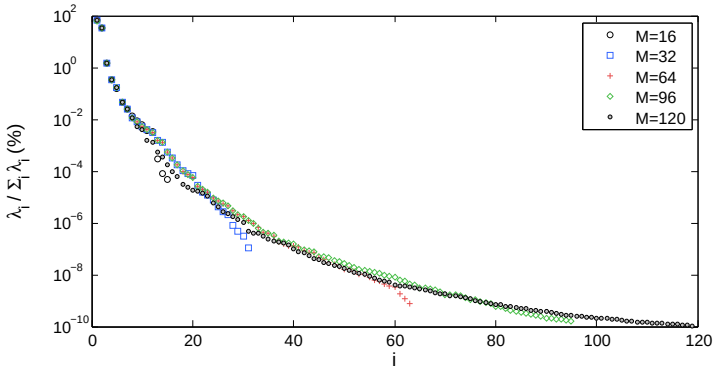

Figure 4: Percentage of energy captured by each eigenvalue λ_i associated to the POM $\boldsymbol{\varphi}^{(i)}$ computed for the NACA0064 example. Several dimensions M of the snapshots set are investigated.

The percentage of energy captured by the POMs is represented on figure 4 for different numbers of snapshots. The sampling time interval $[t_0; t_0 + T_s]$ has also been increased in one case ($M = 120$) to cover about 2.5 periods of the oscillation. The slope of the

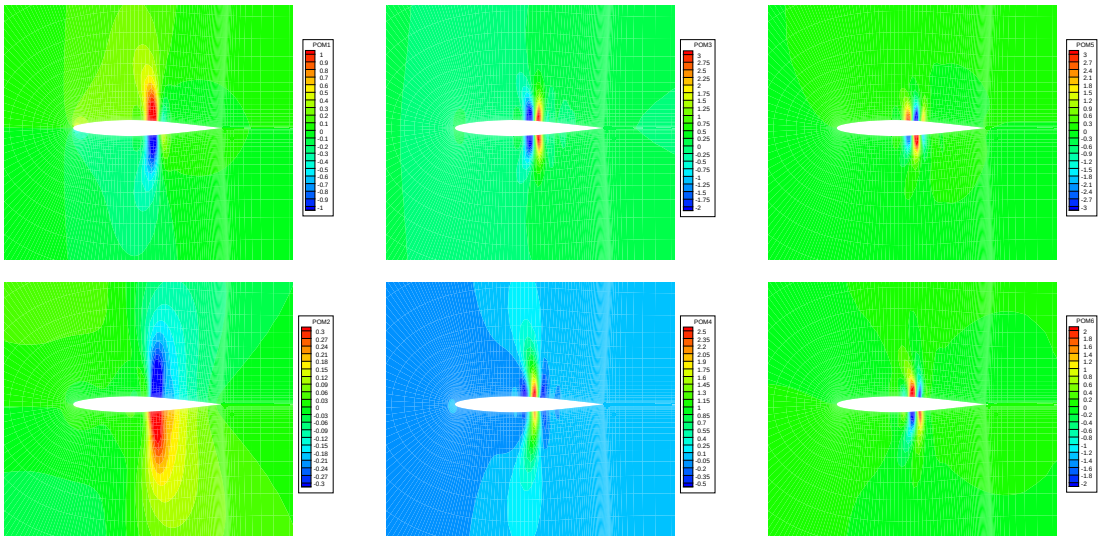

Figure 5: Shape of the first six pressure POMs $\varphi_p^{(i)}$ $(i = 1, \ldots, 6)$ of the flow field around the NACA0064 oscillating airfoil. $M = 120$ snapshots have been used.

spectrum is less steep than in the previous example, but only few POMs can still be kept in the truncated POD basis. The shock-like structure of the transonic flow is revealed by the POMs represented on Figure 5. These POMs are clearly different from the previous example although in both case the flow around an airfoil is considered. This illustrates the strong dependence of the POMs on the application considered: this POD basis is optimal to represent the features of this particular transonic flow field but would be utterly inappropriate to treat the previous example with vortex shedding.

The POD-Galerkin ROM constructed with $q = 10$ POMs and $M = 64$ snapshots is very unstable. This can be explained by the absence of any dissipation in the ROM since the equations from which the ROM is constructed are the Euler equations without artificial dissipation. The corrections used previously for the NACA0012 airfoil are only effective for the short-term behavior: after the sampling time interval, the ROM converges towards erroneous limit cycles or diverges (see Figure 6, left). The correction of Cazemier et al. [5] is too simplistic for the aeroelastic ROM since only the linear diagonal terms are modified. Consequently the correction of Couplet et al. [6] is used in order to calibrate more coefficients of the ROM. However, even with a complex calibration involving constant and diagonal terms (`KdL`), constant terms and linear terms of the three main diagonals (`K3dL`) but also the moving frame coefficients (`KdL_E`), the long term behavior of the ROM response remains unstable or converges towards a wrong attractor. The stability of the system is not improved when the size of the projection basis or the sampling time interval is increased (see Figure 6, right, with $M = 120$ snapshots over about 2.5 periods).

A second ROM is therefore built by means of the POD-based Galerkin-free approach. In this case, no correction is needed and the ROM provides the right limit cycle for the aerodynamic forces as long as the SVD involved to compute the pseudo-inverse has been correctly truncated, i.e. the smallest eigenvalues have been discarded. The result of the time integration of the ROM is presented on the right of Figure 6 and is compared to the response of the POD-Galerkin ROM corrected with `KdL`. In this case, $M = 120$ snapshots have been used so that $M > 1 + q + q^2$ for $q = 10$ and the problem is actually over-determined. The computational cost of the ROM construction and the time savings are presented in Table 1.

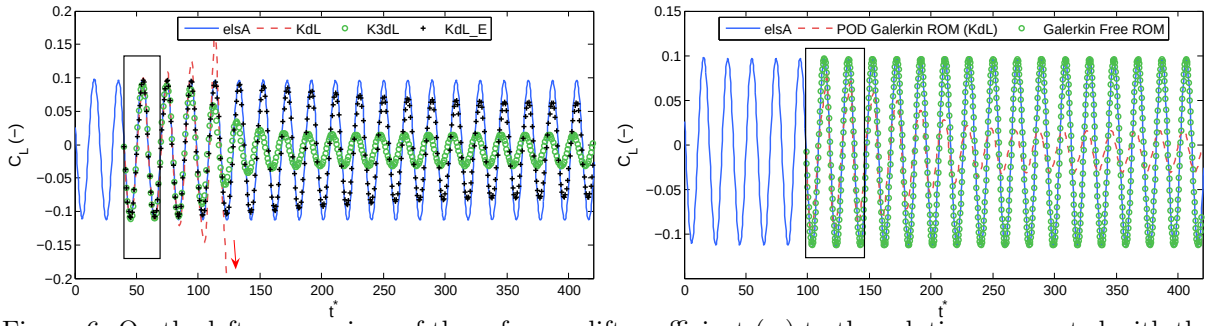

Figure 6: On the left, comparison of the reference lift coefficient (−) to the solutions computed with the POD-Galerkin ROM corrected with `KdL` (− −), with `K3dL` (∘) or with `KdL_E` (+). On the right, the reference response (−) is compared to the response of the Galerkin-free ROM (∘) and the response of the POD-Galerkin ROM corrected with `KdL`. The black rectangles represent the sampling time interval.

5 CONCLUSION

In this paper, ROMs of the Navier-Stokes equations have been developed on the basis of the POD method to reproduce the aerodynamic forces applied on airfoils in fixed or rigidly moving domains. First, a classical POD-Galerkin projection procedure has been used to obtain the small set of ODEs describing the ROM. An accurate response is obtained after the introduction of a correction to make up for the problem of dissipation. Encouraging results have been obtained for the NACA0012 example, but the same approach used for the aeroelastic example with the NACA0064 airfoil demonstrates the limitations of the method for long-term integration: the response of the ROM either diverges or converges towards an erroneous limit cycle, even when a complex calibration is performed. A POD-based Galerkin-free approach has therefore been developed for the second example. The procedure is much less time-consuming and is able to reproduce the right attractor of the system even for long-term time integration. Both types of ROMs provide responses in very few seconds and the CPU time savings are significant. The construction of the ROM is however costly and can be even more time-consuming than the time integration of the high-order model. The use of ROMs is therefore only interesting when many responses for different parameter values can be obtained with the same ROM, i.e. a ROM for which the coefficients have been computed once for all simulations. Future work will deal with the adaptation of the ROM to the modification of the rigid body motion parameters. Indeed, a very accurate response has been obtained here since the validation was performed on the response already computed with the high order model for the same parameter. The response to another set of parameter will certainly not be so accurate and additional techniques like interpolations between POD basis [18] could be used to obtain the response of the system over a certain parameter range.

6 REFERENCES

[1] E. H. Dowell, K.C. Hall, J.P. Thomas, R. Florea, B.I. Epureanu and J. Hegg, *"Reduced order models in unsteady aerodynamics"*, AIAA Paper 99-1261, 40th AIAA Structures, Structural Dynamics and Materials Conference, St. Louis, MO, 1999.

[2] D.J. Lucia, P.S. Beran and W.A. Silva, "Reduced-order modeling: New approaches for computational physics", *Progress in Aerospace Science*, Vol. 40, 2004, pp. 51–117.

[3] J.L. Lumley, "The Structures of Inhomogeneous Turbulent Flow", *In: Atmospheric Turbulence and Radio Wave Propagation*, 1967, pp. 166–178.

[4] D. Rempfer, "Investigations of boundary layer transition via Galerkin projections on empirical eigenfunctions", *Physics of Fluids*, Vol. 8, No. 1, 1996, pp. 175–188.

[5] W. Cazemier, R.W. Verstappen and A.E.P. Veldman, "Proper orthogonal decomposition and low dimensional models for driven cavity flows", *Physics of Fluids*, Vol. 10, No. 7, 1998, pp. 1685–1699.

[6] M. Couplet, C. Basdevant and P. Sagaut, "Calibrated reduced-order POD-Galerkin system for fluid flow modelling", *Journal of Computational Physics*, Vol. 207, No. 1, 2005, pp. 192–220.

[7] S. Sirisup and G.E. Karniadakis, "A spectral viscosity method for correcting the long-term behavior of POD modes", *Journal of Computational Physics*, Vol. 194, No. 1, 2004, pp. 92–116.

[8] A. Iollo, S. Lanteri and J.-A. Désidéri, "Stability properties of POD-Galerkin approximations for the compressible Navier-Stokes equations", *Theoretical and Computational Fluid Dynamics*, Vol. 13, No. 6, 2000, pp. 377–396.

[9] C.W. Rowley, T. Colonius and R.M. Murray, "Model reduction for compressible flows using POD and Galerkin projection", *Physica D*, Vol. 189, 2004, pp. 115–129.

[10] B.I. Epureanu, E.H. Dowell and K.C. Hall, "Reduced-order models of unsteady transonic viscous flows in turbomachinery", *Journal of Fluids and Structures*, Vol. 14, No. 8, 2000, pp. 1215–1234.

[11] T. Lieu, C. Farhat and M. Lesoinne, "Reduced-order fluid/structure modeling of a complete aircraft configuration", *Computer Methods in Applied Mechanics and Engineering*, Vol. 195, No. 41–43, 2006, pp. 5730–5742.

[12] J. Donea, A. Huerta, A., J.-Ph. Ponthot and A. Rodrìguez-Ferran, *Encyclopedia of Computational Mechanics, Vol. 1: Fundamentals, Chap. 14: Arbitrary Lagrangian-Eulerian Methods* John Wiley & Sons, 2004.

[13] M. Gazaix, A. Jolles and M. Lazareff, *"The elsA object-oriented computational tool for industrial applications"*, 23rd Congress of the International Council of the Aeronautical Sciences, September 8-13, Toronto.

[14] P. Holmes, J.L. Lumley and G. Berkooz, *Turbulence, Coherent Structures, Dynamical Systems and Symmetry.* Cambridge University Press, 1996.

[15] A. Placzek, D.-M. Tran and R. Ohayon, "Hybrid proper orthogonal decomposition formulation for linear structural dynamics", *Journal of Sound and Vibration*, Vol. 318, No. 4–5, 2008, pp. 943–964.

[16] L. Sirovich, "Turbulence and the dynamics of coherent structures, Parts I–III", *Quarterly of Applied Mathematics*, Vol. XLV, 1987, pp.561–590.

[17] L. Perret, E. Collin and J. Delville, "Polynomial identification of POD based low-order dynamical system", *Journal of Turbulence*, Vol. 7, No. 17, 2006, pp. 1–15.

[18] C. Farhat and D. Amsallem, *"Recent advances in reduced-order modeling and application to nonlinear computational aeroelasticity"*, 46th AIAA Aerospace Sciences Meeting and Exhibit, Reno, Nevada, 2008.